ISSN (Print) 1226-1750
ISSN (Online) 2233-6656
Journal of Magnetics 24(2), 262-270 (2019) https://doi.org/10.4283/JMAG.2019.24.2.262

MHD Flow of Brinkman Type H_2O-Cu, Ag, TiO_2 and Al_2O_3 Nanofluids with Chemical Reaction and Heat Generation Effects in a Porous Medium

Arshad Khan[1], Dolat Khan[2], Ilyas Khan[3]*, Farhad Ali[2], Faizan ul Karim[2], and Kottakkaran Sooppy Nisar[4]

[1]*Institute of Business and Management Sciences, The University of Agriculture Peshawar, Pakistan*
[2]*Department of Mathematics, City University of Science and Information Technology, Peshawar, 25000, Pakistan*
[3]*Faculty of Mathematics and Statistics, Ton Duc Thang University, Ho Chi Minh City 72915, Vietnam*
[4]*Department of Mathematics, College of Arts and Sciences Wadi Aldawaser, Prince Sattam bin Abdulaziz University, 11991, Saudi Arabia*

(Received 4 July 2018, Received in final form 5 February 2019, Accepted 27 February 2019)

This paper studies magnetohydrodynamic (MHD) flow of Brinkman type nanofluids with the influence of heat generation, chemical reaction and thermal radiation. The fluid is taken over a vertical plate flat passing through a porous medium. Four distinct types of nano particles (Cu, Ag, TiO_2 and Al_2O_3) are taken in a base fluid H_2O. The vertical plate with constant temperature is oscillating in its own plane. The flow is described by the partial deferential equations with suitable initial and boundary conditions. The Laplace transform method is used to obtain the exact solutions for velocity, temperature and concentration. These solutions are interpreted graphically using computational software Mathcad-15 to analyze the influence of embedded parameters such as Brinkman parameter, permeability of porous medium, chemical reaction parameter, nano particle volume fraction, heat generation parameter, magnetic parameter and radiation parameter. Skin-friction, Sherwood number and Nusselt number are calculated mathematically.

Keywords : Nanofluid, Brinkman fluid, nano-particles, porous medium, heat generation

1. Background

Mostly substances of industrial significance such as paint, pharmaceutical and cosmetics, asphalt, glue, particularly of multi-phase nature, polymeric melts are called as non-Newtonian fluids [1, 2]. There are various types of characteristics which led to much excitement of non-Newtonian fluids. Therefore, the behavior of non-Newtonian fluid is more valuable than the Newtonian fluid behavior in nature as well as in technology. Each non-Newtonian fluid has its own complex nature. Due to which several non-Newtonian fluids model have been suggested in literature. The Brinkman fluid model is one of them. Darcy's was proposed model for a problem of examining the effect of boundary layer inserted in a porous medium [3]. This model applies to a body flow with less porosity. Darcy's law is not applicable for a high porous surface for this purpose Brinkman suggested a model which is applicable for great holey surfaces [4, 5]. The viscous fluid in porous medium is exactly described by the Brinkman equations for incompressible flow. However, limited researchers have been worked on this kind of Brinkman fluid. Some studies are primarily published on the Brinkman fluid with the effect of mass and heat transfer, while such studies have numerous engineering applications [6-10]. In this work, we will study Brinkman type nanofluids together with mass and heat transfer. Brinkman type nanofluids are made by incorporating nano particles in base fluid in order to develop its thermal conductivity. For the enhancement of thermal conductivity numerous techniques are used in the literature for the fluid suspended by micro, nano or huge size of particles in fluids [11]. For this purpose, the first effective effort was made by Choi *et al*. [12]. In his paper, he used the nano scaled particles (less than 100 nm) in a base fluid to improve thermal conductivity. This combination of nano particle in a base fluid is termed as nanofluid. Nanofluids have various applications as automotive, power plant cooling, improving diesel generator efficiency etc. [13-20].

*Corresponding author: Tel: +923339022886
e-mail: ilyaskhan@tdtu.edu.vn

Loganathan *et al*. [21] achieved first time particular solution for nanofluids with free convection flow. Madhava Reddy Ch *et al.* [22] studied the combine analysis of heat as well as thermal radiation with unsteady convection flow of Brinkman fluid in a porous medium with chemically reacting. They also studied the dimensionless local skin-friction for Brinkman fluid with porous medium.

Heat transfer passing through a section with absorption and generation effects of heat of nanofluid is studied by Kasmani *et al*. [23]. The influence of chemical reaction with thermal radiation on MHD flow in the existence of heat generation is considered by Shit *et al.* [24]. Das [25] used a numerical technique to observe the MHD flow for nanofluid which is electrically conducting and passes over a perpendicular, permeable extending surface and the existence of chemical reaction. He originates that the concentration of nanofluid shows the decreasing effect on chemical reaction parameter. Ali *et al.* [32] investigated the Solutions with special functions for time fractional free convection flow of Brinkman-type fluid. Furthermore, Engine oil based brinkman-type nano-liquid is investigated by Jan *et al.* [33]. He found a generalized solution by using Atangana-Baleanu fractional model with molybdenum disulphide nanoparticles of spherical shape. Kuznetsov and Nield [34] studded the Thermal instability in a porous medium layer saturated by a nanofluid by using Brinkman model. Hydro magnetic stability of metallic nanofluids (Cu-water and Ag-Water) by using Darcy-Brinkman model is investigated by Ahuja *et al.* [35].

Uddin *et al*. [26] studied theoretically two-dimensional MHD incompressible viscous free convection boundary layer flow of nanofluid which is electrically accompanying with chemical concentration past vertical surface. They also analyzed the effect of several parameters on velocity and chemical profile. The heat transfer effect is investigated by Mohyud-Din *et al.* [27] furthermore the same author is investigated the MHD fluid in parallel disks in [28]. The combined effects of thermal conductivity and diffusivity on nanofluid using spherical and cylindrical types of nano particles are investigated by Xing Zhang *et al.* [29]. They took some specific types of nano particles i.e (Al_2O_3, TiO_2, CuO, CNT) with water and toluene as a base fluid. Moreover, the instantaneous chemical reactions with mass transfer are taking place in gas-liquid systems, and hence the researchers are attracted towards this field. Chemical reaction is either heterogeneous or homogenous. However, no one is investigating to described the joint analysis of heat generating along with thermal radiation and chemical reaction of brinkman kind of nanofluid through a perpendicular plate surrounded in a porous medium.

Based on the above literature and wide range of applications of nanofluids, until this point, no investigation has been made in the literature to inspect the mutual analysis of thermal radiation, heat generation and chemical reaction on MHD flow of Brinkman sort of nanofluid over vertical plate enclosed in a porous medium. Four kinds of nano particles i.e. (Cu, Ag, TiO_2, Al_2O_3) are considered in H_2O as base fluid to examine the problem under consideration. The exact solution of the problem is obtained by the Laplace transform method. The concentration, temperature and velocity are achieved, and plotted in figures by using Mathcad 15 software with some physical discussion.

2. Mathematical Equations and Solutions

Unsteady incompressible flow of brinkman sort of nanofluid with the semi-unlimited porous space $y > 0$ is deliberated. H_2O is use as a base fluid. Magnetic field is orthogonal to the fluid in order the fluid to be electrically conducting. Fig. 1 is represent Physical model of the flow. The effect of magnetic field is neglecting by assumption of minor magnetic Reynolds number. Mass and heat transfer phenomenon is well thought-out in the incidence of radiation, heat generating term. Initially fluid and plate are remain at rest at $t \le 0$, with constant concentration and temperature C_∞ and T_∞. For time $t > 0$ the concentration and temperature levels linearly raised up to T_w and C_w.

The radiative heat flux q_r can be linearized to:

$$q_r = -\frac{16\sigma^* T_\infty^3 T_y}{3k^*} \tag{1}$$

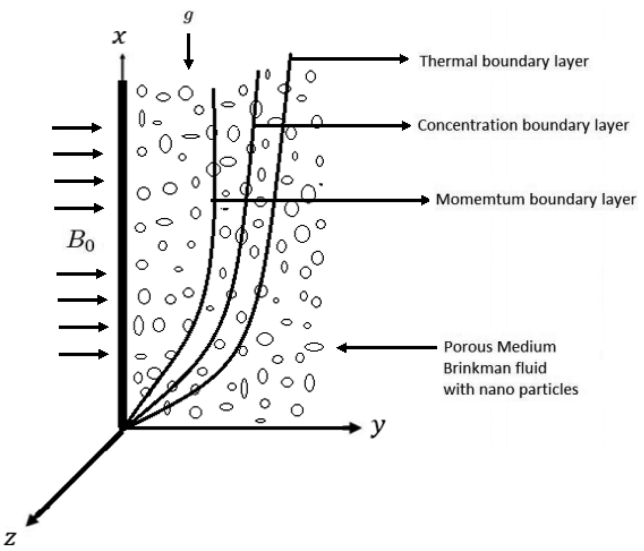

Fig. 1. Physical model of the flow.

where k^* is coefficient of absorption, σ^* is Stefan-Boltzmann constant.

Under the above assumptions and in view of equation (1), we developed the succeeding set of partial differential equations:

$$\rho_{nf}(u_t+\beta u)=\mu_{nf}(u_{yy})-\left(\sigma_{nf}B_0^2+\frac{\mu_{nf}\psi}{k}\right)u +g(\rho\beta_T)_{nf}\left[T-T_\infty\right]+g(\rho\beta_c)_{nf}\left[C-C_\infty\right];\ t,y>0, \tag{2}$$

$$(\rho c_p)_{nf}T_t=k_{nf}\left(1+\frac{16\sigma^*T_\infty^3}{3k_{nf}k^*}\right)T_{yy}+Q_0(T-T_\infty);\ y,t>0 \tag{3}$$

$$C_t=D_{nf}C_{yy}-k_1(C-C_\infty) \tag{4}$$

Initial and boundary conditions are:

$$\left.\begin{array}{l} u=0,\ T=T_\infty,\ C=C_\infty;\ y\geq 0, t=0 \\ u=U\sin(\omega t),\ T=T_w,\ C=C_w;\ t\geq 0, y=0 \\ u\to 0, T\to T_\infty,\ C\to C_\infty \text{ as } y\to\infty. \end{array}\right\}, \tag{5}$$

Here β is the Brinkman parameter, u is indicates the velocity profile of fluid in x-axis path, T is represent temperature and C is represent concentration of fluid, Q_0 is the heat generation term, the density of nanofluids is represent by ρ_{nf}, μ_{nf} is indicates the dynamic viscosity of nanofluid, $\psi(0<\psi<1)$, $k>0$, ψ is porous medium and k is the permeability of porous medium, constant temperature of the plate is denoted by T_w, ($T_w<T_\infty$ or $T_w>T_\infty$) due to the cooled or heated plate, separately), k_1 is represent the chemical parameter and mass diffusivity is denoted by D_{nf}. For nanofluid the expressions of $(\rho c_p)_{nf}$, $(\rho\beta)_{nf}$, μ_{nf}, ρ_{nf}, σ_{nf}, k_{nf} are known as:

$$\begin{aligned} &\rho_{nf}=(1-\varphi)\rho_f+\varphi\rho_s,\ \mu_{nf}=\frac{\mu_f}{(1-\varphi)^{2.5}},\ \sigma=\frac{\sigma_f}{\sigma_s}, \\ &(\rho\beta_c)_{nf}=(1-\varphi)(\rho\beta_c)_f+\varphi(\rho\beta_c)_s, \\ &(\rho\beta_T)_{nf}=(1-\varphi)(\rho\beta_T)_f+\varphi(\rho\beta_T)_s \\ &(\rho c_p)_{nf}=(1-\varphi)(\rho c_p)_f+\varphi(\rho c_p)_s, \\ &k_{nf}=k_f\left(\frac{k_s+2k_f-2\varphi(k_f-k_s)}{k_s+2k_f+\varphi(k_f-k_s)}\right), \\ &\sigma_{nf}=\sigma_f\left(1+\frac{3(\sigma-1)\varphi}{(\sigma+2)-(\sigma-1)\varphi}\right),\ D_{nf}=(1-\phi)D_f, \end{aligned} \tag{6}$$

Table 1. Properties (Thermophysical) of nanofluids [31].

	ρ (kgm^{-3})	c_p (kg^{-1}k^{-1})	k (Wm^{-1}k^{-1})	$\beta\times 10^{-5}$ (k^{-1})
H_2O	997.1	4179	0.613	21
Al_2O_3	3070	765	40	0.85
Cu	8933	385	401	1.67
TiO_2	4250	686.2	8.9528	0.9
Ag	10500	235	429	1.89

where φ the volume fraction of nanoparticles, $(\beta_T)_{nf}$ indicates the thermal expansion coefficient, $(\beta_c)_{nf}$ indicates the coefficient of concentration, density of base fluid and particle is denoted by ρ_f, ρ_s. c_p indicates the specific heat. k_{nf}, k_f, and k_s represent the thermal conductivities of the nanofluid, base-fluid, and solid particles respectively. The expressions in equation (6) are classified to nano particles [30]. For supplementary nano particles with unlike dynamic viscosity, thermal conductivity, see to Table 1 [31].

Interpolating elements for non-dimensional,

$$\upsilon=\frac{u}{U_0},\ \xi=\frac{U_0}{\nu}y,\ \tau=\frac{U_0^2}{\nu}t,\ \theta=\frac{\Theta-\Theta_\infty}{\Theta_w-\Theta_\infty},\ \phi=\frac{C-C_\infty}{C_w-C_\infty}. \tag{7}$$

By using the beyond dimensionless variables into equations (2)-(5), we get the following dimensionless equations

$$\upsilon_\tau=\frac{1}{\mathrm{Re}}\upsilon_{\xi\xi}-H\upsilon+Gr_0\theta+Gm_0\phi\quad \tau,\xi>0, \tag{8}$$

$$c_1\theta_\tau=c_2\theta_{\xi\xi}+c_5\delta\theta;\quad \xi,\tau>0 \tag{9}$$

$$\phi_\tau=\frac{1}{Sc}\phi_{\xi\xi}-\eta\phi;\ \xi,\tau>0 \tag{10}$$

The dimensionless form of initial and boundary conditions are

$$\left.\begin{array}{l} \upsilon=0,\ \theta=0,\ \phi=0;\xi\geq 0,\tau=0 \\ \upsilon=\sin(\omega\tau),\ \theta=1,\ \phi=1;\tau\geq 0,\xi=0 \\ \upsilon\to 0,\ \theta\to 0,\ \phi\to 0 \text{ as } \xi\to\infty. \end{array}\right\} \tag{11}$$

where

$$c_1=1-\varphi+\varphi\frac{(\rho c_p)_s}{(\rho c_p)_f},\ c_2=\frac{\lambda_{nf}(1+Nr)}{\mathrm{Pr}},\ \delta=\frac{\nu Q_0}{U_0^2(\rho c_p)_f},\ \lambda_{nf}=\frac{k_{nf}}{k_f}$$

$$c_3=\frac{(1-\varphi)\rho_f-\varphi\rho_s\left(\frac{\beta_{Tf}}{\beta_{Ts}}\right)}{\rho_{nf}},\ c_4=\frac{(1-\varphi)\rho_f-\varphi\rho_c\left(\frac{\beta_{cf}}{\beta_{cs}}\right)}{\rho_{nf}},\ Sc=\frac{\nu}{(1-\phi)D_f}$$

$$\mathrm{Re}=(1-\varphi)^{2.5}\left[1-\varphi+\varphi\left(\frac{\rho_s}{\rho_f}\right)\right],\ c_5=1+\frac{3(\sigma-1)\varphi}{(\sigma+2)-(\sigma-1)\varphi},$$

$$M=\frac{\sigma_f\nu B_0^2}{\rho_{nf}U_0^2},\ Gr=\frac{\nu g\beta_{Tf}}{U_0^3}(\Theta_w-\Theta_\infty),\ \frac{1}{K}=\frac{\nu_{nf}\psi\nu}{kU_0^2},$$

$$H=M+\frac{1}{K}+\beta_1,\ Nr=\frac{16\sigma^*T_\infty^3}{3k_{nf}k^*},\ \mathrm{Pr}=\frac{(\rho c_p)_f}{k_f},$$

$$Gm=\frac{\nu g\beta_{cf}}{U_0^3}(C_w-C_\infty),\ \eta=\frac{k_1\nu}{U_0^2},\ Gr_0=c_3Gr,$$

$$Gm_0=c_4Gm,\ \delta=\frac{\nu Q_0}{U_0^2(\rho c_p)_f},$$

where Re, $\frac{1}{K}$, δ, β_1, Gr, M, Nr, Gm, η, Sc and Pr are Reynolds number, permeability of pours medium, heat generation parameter, dimensionless Brinkman parameter, thermal Grashof number, magnetic parameter, radiation parameter, mass Grashof number, chemical reaction Schmidt number, and Prandtl number respectively.

3. Exact Solution

By applying Laplace transform to Eqs. (8-11), with the transformed boundary conditions and solving the resulting differential equation for the transformed variables $\bar{\theta}(\xi, s)$, $\bar{\phi}(\xi, s)$ and $\bar{\upsilon}(\xi, s)$ in the (ξ, s) −plane, we obtained

$$\bar{\theta}(\xi,s)=\frac{1}{s}\exp\left(-\xi\sqrt{\frac{c_1}{c_2}\left(\frac{\delta}{c_1}-s\right)}\right), \tag{12}$$

$$\bar{\phi}(\xi,s)=\frac{1}{s}\exp\left(-\xi\sqrt{Sc(s+\eta)}\right), \tag{13}$$

$$\bar{\upsilon}(\xi,s)=\bar{\upsilon_i}(\xi,s)+\bar{\upsilon_{ii}}(\xi,s)+\bar{\upsilon_{iii}}(\xi,s)+\bar{\upsilon_{iv}}(\xi,s)+\bar{\upsilon_v}(\xi,s), \tag{14}$$

$$\begin{aligned}
\bar{\upsilon_i}(\xi,s)&=\frac{\omega}{s^2+\omega^2}\exp\left(-\xi\sqrt{\mathrm{Re}(s+H)}\right)\\
\bar{\upsilon_{ii}}(\xi,s)&=\left(\frac{c_5}{c_6}+\frac{c_8}{c_7}\right)\frac{1}{s}\exp\left(-\xi\sqrt{\mathrm{Re}(s+H)}\right)\\
\bar{\upsilon_{iii}}(\xi,s)&=\left(\frac{-c_5}{c_6}\frac{1}{s+c_6}-\frac{c_8}{c_7}\frac{1}{s+c_7}\right)\exp\left(-\xi\sqrt{\mathrm{Re}(s+H)}\right)\\
\bar{\upsilon_{iv}}(\xi,s)&=\frac{c_5}{c_6}\left(\frac{1}{s+c_6}-\frac{1}{s}\right)\exp\left(-\xi\sqrt{\frac{c_1}{c_2}\left(\frac{\delta}{c_1}-s\right)}\right)\\
\bar{\upsilon_v}(\xi,s)&=\frac{c_8}{c_7}\left(\frac{1}{s+c_7}-\frac{1}{s}\right)\exp\left(-\xi\sqrt{Sc(s+\eta)}\right)
\end{aligned} \tag{15}$$

where

$$c_5=\frac{\mathrm{Re}\,Gr_0}{-\frac{c_1}{c_2}-\mathrm{Re}},\ c_6=\frac{\frac{\delta}{c_2}-\mathrm{Re}\,H}{-\frac{c_1}{c_2}-\mathrm{Re}},\ c_7=\frac{Sc\eta-\mathrm{Re}\,H}{Sc-\mathrm{Re}},\ c_8=\frac{\mathrm{Re}\,Gm_0}{Sc-\mathrm{Re}}.$$

After inverse Laplace transform and comprehensive simplifications of the equations (12-14), the solutions can be expressed as:

$$\theta(\xi,\tau)=\frac{1}{2}\left\{\begin{aligned}&\exp\left(-\xi\sqrt{\frac{\delta}{c_2}}\right)erfc\left(\frac{i\xi\sqrt{\frac{c_1}{c_2}}}{2\sqrt{\tau}}+i\sqrt{\frac{\delta}{c_1}\tau}\right)\\&+\exp\left(\xi\sqrt{\frac{\delta}{c_2}}\right)erfc\left(\frac{i\xi\sqrt{\frac{c_1}{c_2}}}{2\sqrt{\tau}}-i\sqrt{\frac{\delta}{c_1}\tau}\right)\end{aligned}\right\}, \tag{16}$$

$$\phi(\xi,\tau)=\frac{1}{2}\left\{\begin{aligned}&\exp\left(\xi\sqrt{Sc}\right)erfc\left(\frac{\xi\sqrt{Sc}}{2\sqrt{\tau}}+\sqrt{\eta\tau}\right)\\&+\exp\left(-\xi\sqrt{Sc}\right)erfc\left(\frac{\xi\sqrt{Sc}}{2\sqrt{\tau}}-\sqrt{\eta\tau}\right)\end{aligned}\right\}, \tag{17}$$

$$\upsilon(\xi,\tau)=\upsilon_i(\xi,\tau)+\upsilon_{ii}(\xi,\tau)+\upsilon_{iii}(\xi,\tau)+\upsilon_{iv}(\xi,\tau)+\upsilon_v(\xi,\tau), \tag{18}$$

where

$$\begin{aligned}
\upsilon_i(\xi,\tau)=&\frac{1}{4\mathrm{i}}\exp(i\tau w)\\
&\left[\begin{aligned}&\exp\left(-\xi\sqrt{\mathrm{Re}(H+\mathrm{i}w)}\right)erfc\left\{\frac{\xi}{2}\sqrt{\frac{\mathrm{Re}}{\tau}}-\sqrt{\tau(H+\mathrm{i}w)}\right\}\\&+\exp\left(\xi\sqrt{\mathrm{Re}(H+\mathrm{i}w)}\right)erfc\left\{\frac{\xi}{2}\sqrt{\frac{\mathrm{Re}}{\tau}}+\sqrt{\tau(H+\mathrm{i}w)}\right\}\end{aligned}\right]\\
&-\frac{1}{4\mathrm{i}}\exp(i\tau w)\\
&\left[\begin{aligned}&\exp\left(-\xi\sqrt{\mathrm{Re}(H-\mathrm{i}w)}\right)erfc\left\{\frac{\xi}{2}\sqrt{\frac{\mathrm{Re}}{\tau}}-\sqrt{\tau(H-\mathrm{i}w)}\right\}\\&+\exp\left(\xi\sqrt{\mathrm{Re}(H-\mathrm{i}w)}\right)erfc\left\{\frac{\xi}{2}\sqrt{\frac{\mathrm{Re}}{\tau}}+\sqrt{\tau(H-\mathrm{i}w)}\right\}\end{aligned}\right]
\end{aligned} \tag{19}$$

$$\upsilon_{ii}(\xi,\tau)=\frac{1}{2}\left(\frac{c_5}{c_6}+\frac{c_8}{c_7}\right)\left\{\begin{aligned}&\exp\left(\xi\sqrt{\mathrm{Re}\,H}\right)erfc\left[\frac{\xi}{2}\sqrt{\frac{\mathrm{Re}}{\tau}}+\sqrt{\tau H}\right]\\&+\exp\left(-\xi\sqrt{\mathrm{Re}\,H}\right)erfc\left[\frac{\xi}{2}\sqrt{\frac{\mathrm{Re}}{\tau}}-\sqrt{\tau H}\right]\end{aligned}\right\} \tag{20}$$

$$\begin{aligned}
\upsilon(\xi,\tau)_{iii}=&\frac{-c_5}{2c_6}\exp(-c_6\tau)\\
&\left\{\begin{aligned}&\exp\left(-\xi\sqrt{\mathrm{Re}(H-c_6)}\right)erfc\left[\frac{\xi}{2}\sqrt{\frac{\mathrm{Re}}{\tau}}-\sqrt{\tau(H-c_6)}\right]\\&+\exp\left(\xi\sqrt{\mathrm{Re}(H-c_6)}\right)erfc\left[\frac{\xi}{2}\sqrt{\frac{\mathrm{Re}}{\tau}}+\sqrt{\tau(H-c_6)}\right]\end{aligned}\right\}\\
&-\frac{c_8}{2c_7}\exp(-c_7\tau)\\
&\left\{\begin{aligned}&\exp\left(-\xi\sqrt{\mathrm{Re}(H-c_7)}\right)erfc\left[\frac{\xi}{2}\sqrt{\frac{\mathrm{Re}}{\tau}}-\sqrt{\tau(H-c_7)}\right]\\&+\exp\left(\xi\sqrt{\mathrm{Re}(H-c_7)}\right)erfc\left[\frac{\xi}{2}\sqrt{\frac{\mathrm{Re}}{\tau}}+\sqrt{\tau(H-c_7)}\right]\end{aligned}\right\}
\end{aligned} \tag{21}$$

$$\begin{aligned}
\upsilon_{iv}(\xi,\tau)=&\\
&\frac{c_5}{c_6}\left\{\begin{aligned}&\frac{1}{2}\exp(c_6\tau)\left\{\begin{aligned}&\exp\left(-\xi\sqrt{\frac{c_1}{c_2}\left(\frac{\delta}{c_1}-c_6\right)}\right)erfc\left[\frac{\xi}{2i}\sqrt{\frac{c_1}{c_2\tau}}-i\sqrt{\left(\frac{\delta}{c_1}-c_6\right)\tau}\right]\\&+\exp\left(\xi\sqrt{\frac{c_1}{c_2}\left(\frac{\delta}{c_1}-c_6\right)}\right)erfc\left[\frac{\xi}{2i}\sqrt{\frac{c_1}{c_2\tau}}+i\sqrt{\left(\frac{\delta}{c_1}-c_6\right)\tau}\right]\end{aligned}\right\}\\&-\frac{1}{2}\left\{\begin{aligned}&\exp\left(\xi\sqrt{\frac{\delta}{c_2}}\right)erfc\left[\frac{\xi}{2i}\sqrt{\frac{c_1}{c_2\tau}}+i\sqrt{\delta\tau}\right]\\&+\exp\left(-\xi\sqrt{\frac{\delta}{c_2}}\right)erfc\left[\frac{\xi}{2i}\sqrt{\frac{c_1}{c_2\tau}}-i\sqrt{\delta\tau}\right]\end{aligned}\right\}\end{aligned}\right\}
\end{aligned} \tag{22}$$

$$\upsilon_v(\xi,\tau)=\frac{c_8}{c_7}\left\{\begin{array}{l}\frac{1}{2}\exp(c_7\tau)\left\{\begin{array}{l}\exp\left(-\xi\sqrt{Sc(\eta+c_7)}\right)erfc\left[\frac{\xi}{2}\sqrt{\frac{Sc}{\tau}}-\sqrt{(\eta+c_7)\tau}\right]\\+\exp\left(\xi\sqrt{Sc(\eta+c_7)}\right)erfc\left[\frac{\xi}{2}\sqrt{\frac{Sc}{\tau}}+\sqrt{(\eta+c_7)\tau}\right]\end{array}\right\}\\-\frac{1}{2}\left\{\begin{array}{l}\exp\left(\xi\sqrt{Sc\eta}\right)erfc\left[\frac{\xi}{2}\sqrt{\frac{Sc}{\tau}}+\sqrt{\eta\tau}\right]\\+\exp\left(-\xi\sqrt{Sc\eta}\right)erfc\left[\frac{\xi}{2}\sqrt{\frac{Sc}{\tau}}-\sqrt{\eta\tau}\right]\end{array}\right\}\end{array}\right\}. \tag{23}$$

4. Skin friction, Nusselt number, Sherwood number

The expression for Nu, C_{fx} and Sh_x are:

$$C_{fx}=\frac{\tau_w x}{\rho_f u_w^2},\ Nu_x=\frac{xq_w}{k(\Theta_w-\Theta_\infty)},\ Sh_x=\frac{xq_s}{D_f(C_w-C_\infty)}, \tag{24}$$

where q_w, τ_w, q_s are the dimensional wall heat flux, shear stress and wall mass flux, represent as:

$$\tau_w=-\mu_{nf}\left(\frac{\partial\upsilon}{\partial\xi}\right)_{\xi=0},\ q_w=-k_{nf}\left(\frac{\partial\Theta}{\partial\xi}\right)_{\xi=0},\ q_s=-D_{nf}\left(\frac{\partial C}{\partial\xi}\right)_{\xi=0}. \tag{25}$$

Using Eqns. (6) and (7), we have from Eqn. (24)

$$\begin{aligned}&\mathrm{Re}_x^{1/2}(1-\phi)^{2.5}C_{fx}=\frac{\partial\upsilon(\xi,\tau)}{\partial\xi}\Big|_{\xi=0}=\\&\frac{1}{2}\mathrm{i}e^{-\mathrm{i}\tau w}\left[\begin{array}{l}\sqrt{\frac{\mathrm{Re}}{\pi\tau}}\left\{\exp\left(-\tau(H+\mathrm{i}w)\right)+\exp\left(-\tau(H-\mathrm{i}w)\right)\right\}\\-erf\left[\tau(H+\mathrm{i}w)\right]+erf\left[\tau(H-\mathrm{i}w)\right]\end{array}\right]\\&-\left(\frac{c_5}{c_6}+\frac{c_8}{c_7}\right)\left\{\sqrt{\frac{\mathrm{Re}}{\pi\tau}}\exp(-H\tau)+erf\left[\sqrt{H\tau}\right]\right\}\\&+\frac{c_5}{c_6}\sqrt{\mathrm{Re}}\exp(-c_6\tau)\left\{\frac{1}{\sqrt{\pi\tau}}\exp\left(-(H-c_6)\tau\right)+erf\left[\sqrt{(H-c_6)\tau}\right]\right\}\\&+\frac{c_8}{c_7}\sqrt{\mathrm{Re}}\exp(-c_7\tau)\left\{\frac{1}{\sqrt{\pi\tau}}\exp\left(-(H-c_7)\tau\right)+erf\left[\sqrt{(H-c_7)\tau}\right]\right\}\\&-\frac{c_5}{c_6}\left\{\begin{array}{l}\exp(c_6\tau)\left\{\sqrt{\frac{c_1}{c_2}}\left\{\frac{-1}{\sqrt{-\pi\tau}}\exp\left(\left(\frac{\delta}{c_1}-c_6\right)\tau\right)-\sqrt{\frac{\delta}{c_1}-c_6}erf\left[-\tau\sqrt{c_6-\frac{\delta}{c_1}}\right]\right\}\right\}\\+\sqrt{\frac{c_1}{-c_2\pi\tau}}\exp(\delta\tau)+\sqrt{\frac{\delta}{c_2}}erf\left[\sqrt{-\delta\tau}\right]\end{array}\right\}\\&-\frac{c_8}{c_7}\sqrt{Sc}\left\{\begin{array}{l}\exp(c_7\tau)\left\{\frac{-1}{\sqrt{\pi\tau}}\exp\left(-(\eta+c_7)\tau\right)-\sqrt{\eta+c_7}erf\left[\tau\sqrt{\eta+c_7}\right]\right\}\\+\frac{1}{\sqrt{\pi\tau}}\exp(-\eta\tau)+\sqrt{\eta}erf\left[\sqrt{\eta\tau}\right]\end{array}\right\}\end{aligned} \tag{26}$$

$$Nu_x=-\frac{k_{nf}}{k_f}\mathrm{Re}_x^{1/2}\frac{\partial\theta(\xi,\tau)}{\partial\xi}\Big|_{y=0}=-2\frac{k_{nf}}{k_f}\mathrm{Re}_x^{1/2}\sqrt{\frac{-c_1}{c_2\pi\tau}}\exp\left(\frac{\delta\tau}{c_1}\right) \tag{27}$$

$$Sh_x=-(1-\phi)\mathrm{Re}_x^{1/2}\frac{\partial\phi(\xi,\tau)}{\partial\xi}\Big|_{\xi=0}=-2(1-\phi)\mathrm{Re}_x^{1/2}\sqrt{\frac{Sc}{\pi\tau}}\exp(-\eta\tau) \tag{28}$$

where $\mathrm{Re}_x=\frac{U_0 x}{\nu_f}$ is local Reynolds number.

5. Results and Discussion

For better understanding the effects of parameters the graphs for $\phi(\xi,\tau)$, $\theta(\xi,\tau)$ and $\upsilon(\xi,\tau)$ are plotted in Figs. 2-18. Brinkman parameter β, volume fraction φ, mass Grashof number Gm,thermal Grashof number Gr, heat generation parameter δ, magnetic parameter M, chemical reaction parameter η, permeability of porous medium k, Schmidt number Sc, Prandtl number Pr, radiation parameter Nr. For computational analysis four different types of nano particles that is Ag, TiO_2, Cu, Al_2O_3 are considered with water as a based fluid. The inspiration of Brinkman parameter β on velocity is highlight in Fig. 2, if the Brinkman parameter is zero then the velocity is greater and increasing Brinkman parameter, decrease the velocity profile. It is due to drag force.

In Figs. 3 and 13 the stimulation of nano particles volume fraction φ on temperature and velocity profile are studied respectively. The range of φ is taken in between 0

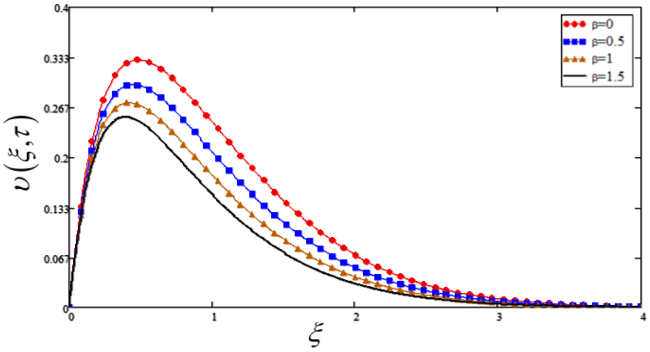

Fig. 2. (Color online) Brinkman parameter β graph for velocity.

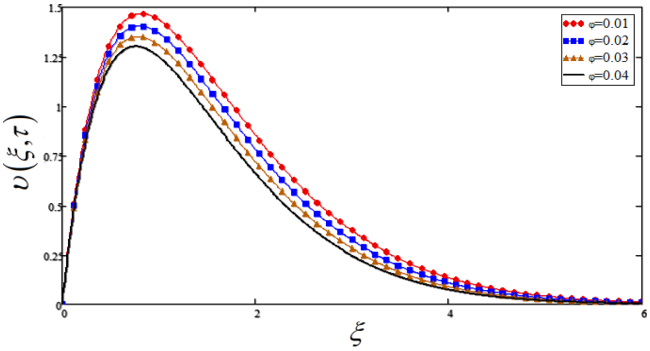

Fig. 3. (Color online) Volume fraction of nanoparticles φ graph for velocity.

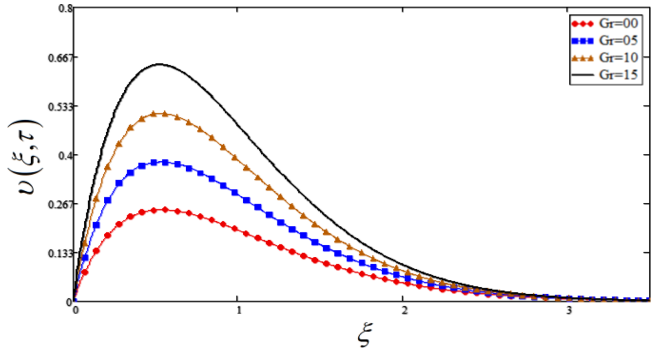

Fig. 4. (Color online) Thermal Grashof number *Gr* graph for velocity.

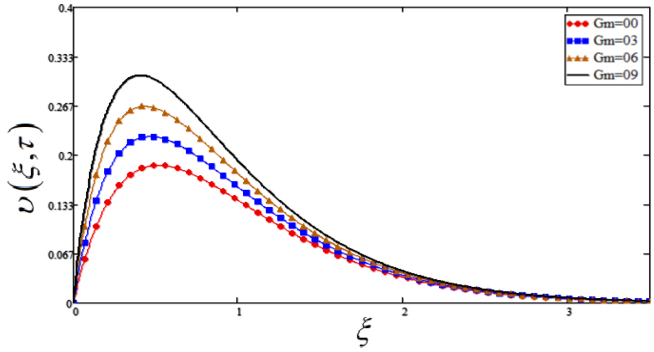

Fig. 5. (Color online) Heat generation parameter *Gm* graph for velocity.

and 0.04. In both cases nano particles volume fraction φ shows a decreasing effect on temperature and velocity profiles which shows the application of nano particles in Brinkman type fluid.

Figure 4 highlights the influence of thermal Grashof number *Gr* and in Fig. 5 the effect of mass Grashof number *Gm* is highlighted. Both graphs show identical behavior on velocity profile that velocity increases with increasing *Gr* and *Gm*. However, the thermal Grashof number *Gr* shows more increasing effect on velocity as compare to that of mass *Gm*. It is because of buoyancy

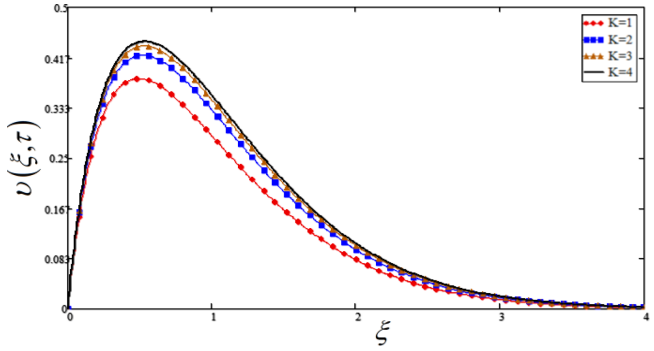

Fig. 6. (Color online) Permeability of pours medium *K* graph for velocity.

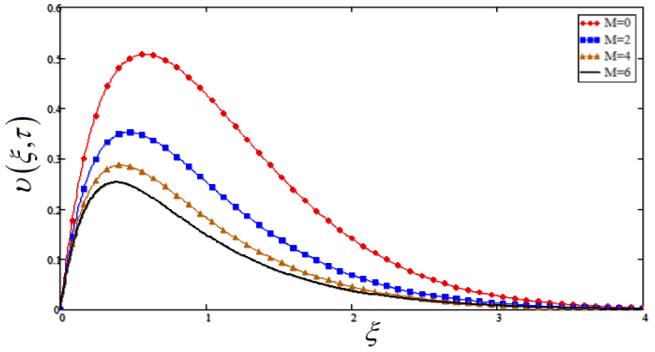

Fig. 7. (Color online) Magnetic parameter *M* graph for velocity.

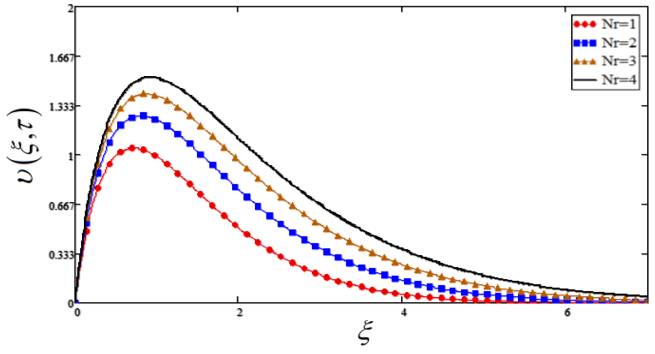

Fig. 8. (Color online) Radiation parameter *Nr* graph for velocity.

force which enhance the temperature and concentration gradients. The influence of permeability of porous medium *K* and magnetic parameter *M* on velocity profile is shown in Figs. 6 and 7. Opposite behavior of *M* and *K* is noted. The permeability of pours medium *K* increases the velocity and magnetic parameter *M* shows reducing effect on velocity with increasing values of *M*. The stimulation of radiation parameter *Nr* on velocity and temperature profile is studied in Figs. 8 and 16. Rising in radiation parameter *Nr* shows arise in temperature and leads to the increasing velocity profile. The significance of Prandtl

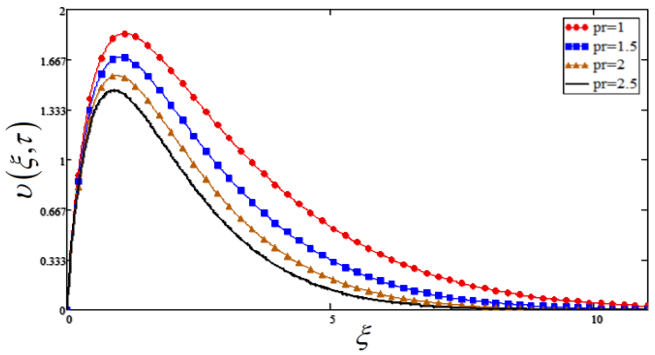

Fig. 9. (Color online) Prandtl number *Pr* graph for velocity.

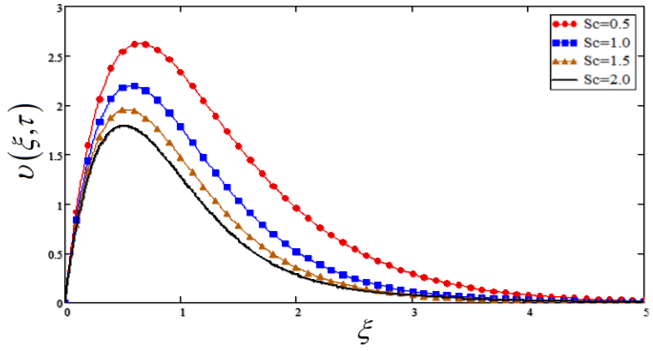

Fig. 10. (Color online) Schmidt number *Sc* graph for velocity.

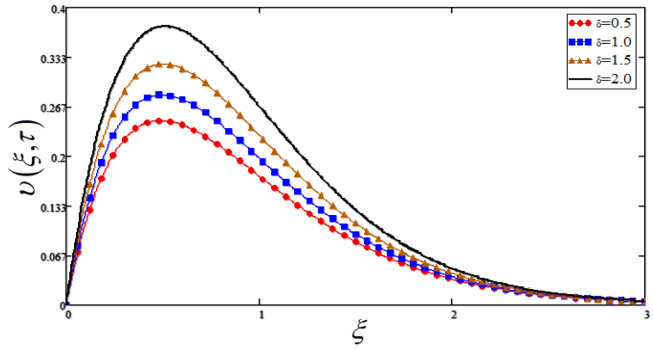

Fig. 11. (Color online) Mass Grashof number δ graph for velocity.

number Pr on velocity and temperature profile is studied in Figs. 9 and 14. Increasing Prandtl number Pr shows a decreasing effect on velocity and temperature. The influence of Schmidt number *Sc* is reported in Figs. 10 and 17 for both velocity and concentration profile, the concentration boundary layer thickness is reduced for a large value of *Sc*, which leads to the decreasing velocity and concentration profiles.

Figures 11 and 15 highlight the inspiration of heat generation parameter δ on both the velocity and temperature profiles. An identical behavior is noted. It is due to heat absorption.

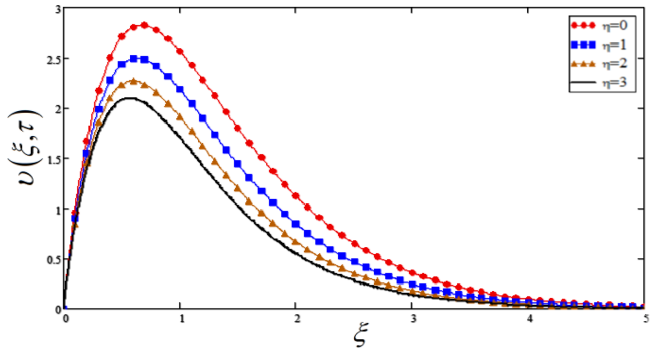

Fig. 12. (Color online) Chemical reaction parameter η graph for velocity.

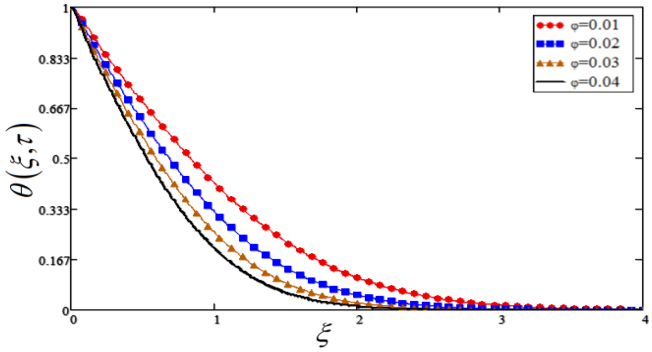

Fig. 13. (Color online) Volume fraction of nanoparticles φ graph for temperature.

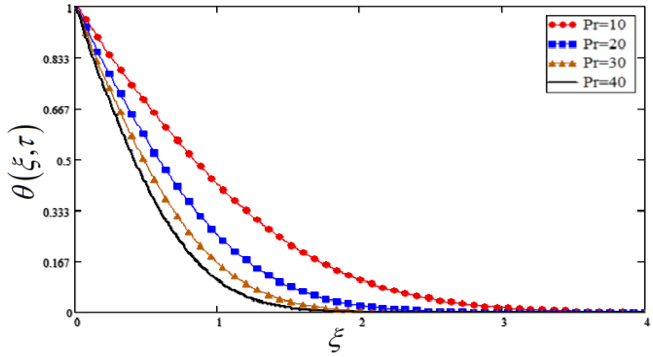

Fig. 14. (Color online) Prandtl number Pr graph for temperature.

In Figs. 12 and 18, it is detected that an upturn in chemical reaction parameter η, decrease the velocity along concentration profiles. Actually it is really true because when η rises this leads to a reduction in the concentration and, finally reductions is occur in velocity profile.

A comparison of the four different sorts of nanofluids namely H_2O-Ag, H_2O-Cu, H_2O-TiO_2 and H_2O-Al_2O_3 is given in Fig. 19 for not the same values of nanoparticles volume fraction parameter φ. It is bring into being that H_2O-Al_2O_3 have greater velocity as compare to other

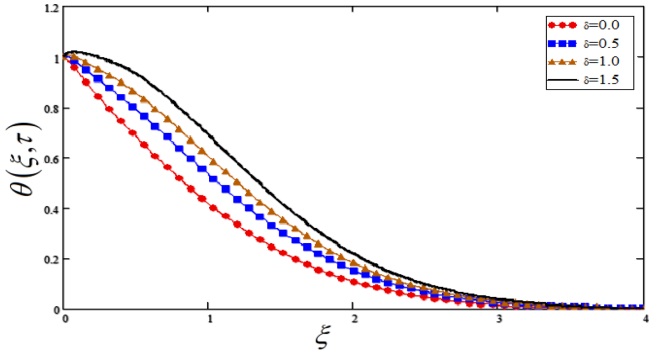

Fig. 15. (Color online) Heat generation parameter δ graph for temperature.

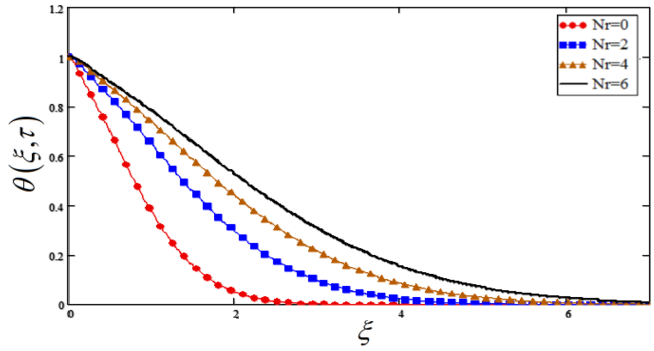

Fig. 16. (Color online) Radiation parameter *Nr* graph for temperature.

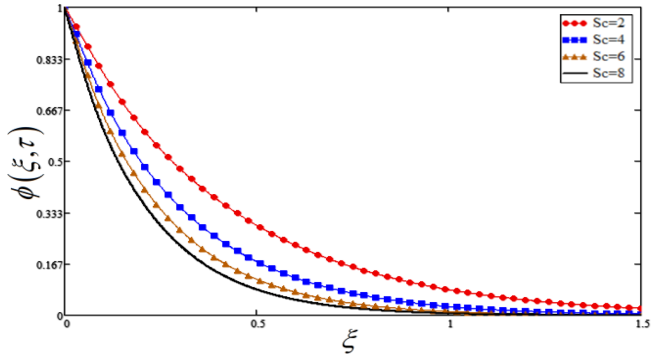

Fig. 17. (Color online) Concentration plot for Schmidt number *Sc*.

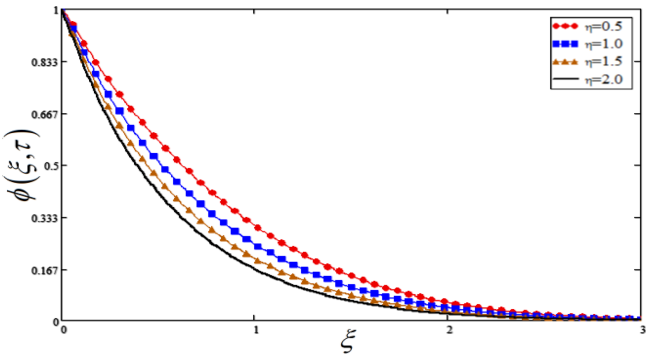

Fig. 18. (Color online) Concentration plot for chemical reaction parameter η.

nano particles. It is physically true that Al_2O_3 nano particles have high thermal diffusivity as compare to other nano particles. Therefore velocity profile is greater.

6. Conclusion

The performance of MHD flow of chemical reaction, heat generation with thermal radiation effect on Brinkman sort of nanofluid in excess of perpendicular plate in a porous medium is studied. The exact solution of velocity, concentration and temperature profile is gained by using Laplace transform. Specific important results are listed

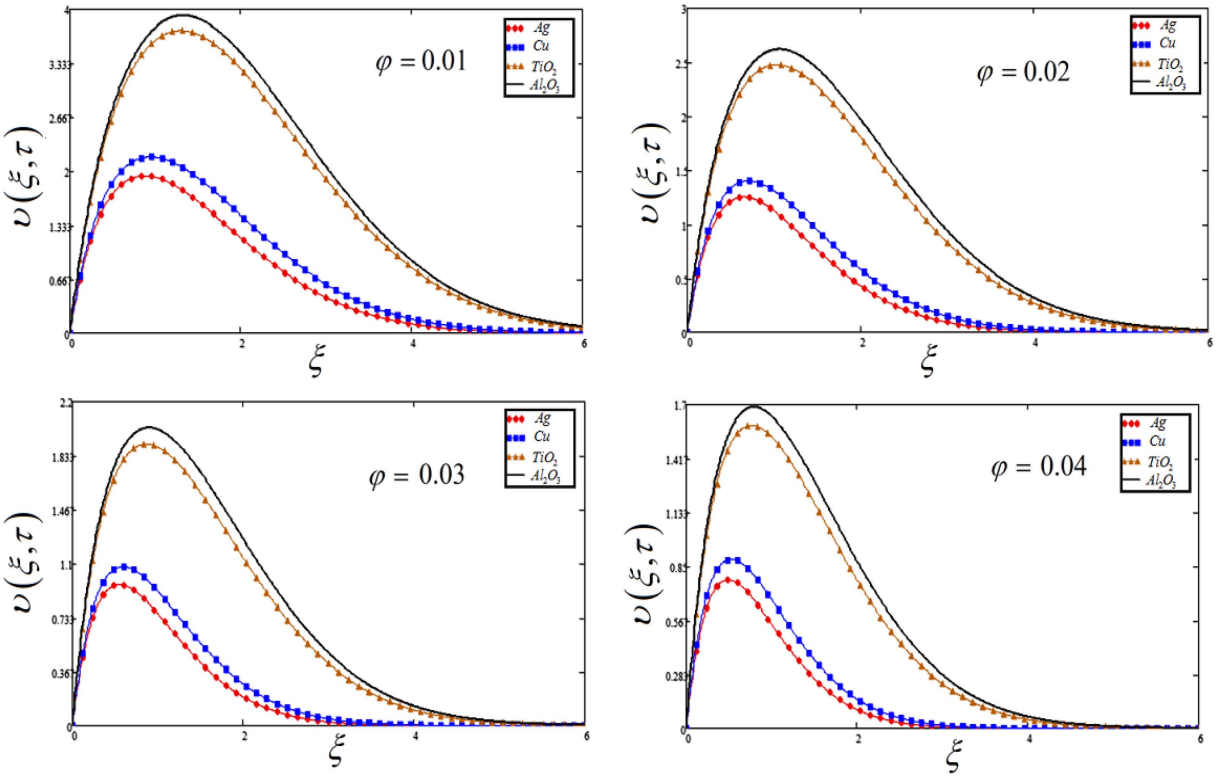

Fig. 19. (Color online) Comparison of velocities plot of nanofluids.

here.

• Brinkman parameter β prompts diminish the velocity profile.

• Both the mass and thermal Grashof number *Gm*, *Gr* increases the profile velocity.

• Thermal Grashof number *Gr* has greater effect then mass Grashof number *Gm*.

• The velocity growths with increasing K, Gr, Gm, Nr, δ and drop with decreasing φ, *M*, Pr, *Sc*, η.

• The effect of Al_2O_3 shows greater velocity profile as compare to other nano particles.

Acknowledgments

The authors thank the editor and anonymous reviewers for their constructive comments, which helped us to improve the manuscript.

Competing Interests

The authors declare that they have no competing interests.

References

[1] A. Aliseda, E. J. Hopfinger, J. C. Lasheras, D. M. Kremer, A. Berchielli, and E. K. Connolly, Int. J. Multiph. Flow. **34**, 161 (2008).
[2] K. J. Lissant, 4,040,857 (1977).
[3] H. Darcy, Les fontaines publiques de la ville de Dijon: exposition et application... Victor Dalmont (1856).
[4] H. C. Brinkman, Flow Turbul. Combust. **1.1**, 81 (1949).
[5] Neale, Graham, and Walter Nader, Can. J. Chem. Eng. **52.4**, 475 (1974).
[6] C. Lin and L. E. Payne, Math. Method. Appl. Sci. **30**, 567 (2007).
[7] A. A. Hill, Continuum. Mech. Therm. **16**, 43 (2004).
[8] C. Fetecau, C. Fetecau, and M. A. Imran, Math. Reports **13**, 15 (2011).
[9] A. Farhad, I. Khan, and S. Shafie, Naturforsch. A **67**, 377 (2012).
[10] M. N. Zakaria, A. Hussanan, I. Khan, and S. Shafie, J. Teknologi. **62**, 33 (2013).
[11] S. Kakac and A. Pramuanjaroenkij, Int. J. Heat Mass Transf. **52**, 3187 (2009).
[12] S. U. S. Choi, ASME-Publications-Fed **231**, 99 (1995).
[13] R. U. Haq, S. Nadeem, Z. H. Khan, and N. F. M. Noor, Physica E. Low. Dimens Syst. Nanostruct. **73**, 45 (2015).
[14] S. T. Hussain, Z. H. Khan, and S. Nadeem, J. Mol. Liq. **214**, 136 (2016).
[15] R. U. Haq, D. Rajotia, and N. F. M. Noor, Eur. Phys. J. E **39**, 1 (2016).
[16] A. Khalid, I. Khan, and S. Shafie, Eur. Phys. J. Plus. **130**, 1 (2015).
[17] S. U. Rehman, R. U. Haq, Z. H. Khan, and C. Lee, J. Taiwan. Inst. Chem. Eng. **63**, 226 (2016).
[18] R. Kandasamy, R. Mohamad, and M. Ismoen, Eng. Sci. Technol. Int. J. **1**, 1 (2015).
[19] R. U. Haq, N. F. M. Noor, and Z. H. Khan, Adv. Powder. Technol. **27**, 1568 (2016).
[20] Z. H. Khan, S. T. Hussain, and Z. Hammouch, J. Mol. Liq. **221**, 298 (2016).
[21] P. Loganathan, P. Nirmal Chand, and P. Ganesan, Nano **8**, 135000 (2013).
[22] M. R. Ch, T. K. V. Iyengar, and K. Gandhi, Procedia Eng. **127**, 140 (2015).
[23] R. M. Kasmani, S. Sivasankaran, M. Bhuvaneswari, and Z. Siri, J. Appl. Fluid. Mech. **9**, 1 (2016).
[24] G. C. Shit, and S. Majee, J. Appl. Fluid. Mech. **7**, 239 (2014).
[25] K. Das, J. Comput. Appl. Math. **221**, 547 (2013).
[26] M. J. Uddin, O. A. Bég, A. Aziz, and A. I. Ismail, Math. Probl. Eng. **1**, 32 (2015).
[27] S. T. Mohyud-Din, Z. A. Zaidi, S. I. U. Khan, and X. J. Yang, Non. Sci. Let. Mater. Phys. Mech. **61**, 71 (2012).
[28] S. T. Mohyud-Din, S. I. Khan, U. Khan, N. Ahmed, and Y. Xiao-Jun, Aerosp. Sci. Technol. **1**, 514 (2017).
[29] X. Zhang, H. Gu, and M. Fujii, Exp. Therm. Fluid. Sci. **31**, 593 (2007).
[30] S. T. Hussain, Z. H. Khan, and S. Nadeem, J. Mol. Liq. **214**, 136 (2016).
[31] A. Khalid, I. Khan, and S. Shafie, Eur. Phys. J. Plus. **130**, 1 (2015).
[32] F. Ali, S. A. A. Jan, I. Khan, M. Gohar, and N. A. Sheikh, Eur. Phys. J. Plus. **131**, 310 (2016).
[33] S. A. A. Jan, F. Ali, N. A. Sheikh, I. Khan, M. Saqib, and M. Gohar, Numer. Methods. Partial. Differ. Equ. **34**, 1472 (2018).
[34] A. V. Kuznetsov and D. A. Nield, Transport. Porous. Med. **81**, 409 (2010).
[35] J. Ahuja, U. Gupta, and R. K. Wanchoo, J. Int. 2016 (2016).